Received: 1 August 2023 | Revised: 11 December 2023 | Accepted: 2 January 2024

DOI: 10.1002/biot.202300381

Biotechnology Journal

RESEARCH ARTICLE

Identification of critical process parameters for expansion of clinical grade human Wharton's jelly-derived mesenchymal stromal cells in stirred-tank bioreactors

Alba López-Fernández[1] | **Víctor Garcia-Gragera**[1,2] | **Martí Lecina**[2] | **Joaquim Vives**[1,3,4]

[1]Servei de Teràpia Cel·lular i Avançada, Banc de Sang i Teixits, Edifici Dr. Frederic Duran i Jordà, Barcelona, Spain

[2]Engineering Materials Group (GEMAT), Bioprocessing Lab, IQS School of Engineering, Universitat Ramón Llull, Barcelona, Spain

[3]Musculoskeletal Tissue Engineering Group, Vall d'Hebron Research Institute (VHIR), Universitat Autònoma de Barcelona, Barcelona, Spain

[4]Departament de Medicina, Universitat Autònoma de Barcelona, Barcelona, Spain

Correspondence
Martí Lecina, Engineering Materials Group (GEMAT), Bioprocessing Lab, IQS School of Engineering, Universitat Ramón Llull, Barcelona, 08017, Spain.
Email: marti.lecina@iqs.url.edu

Joaquim Vives, Servei de Teràpia Cel·lular i Avançada, Banc de Sang i Teixits, Edifici Dr. Frederic Duran i Jordà, Passeig Taulat, 116, 08005 Barcelona, Spain.
Email: jvives@bst.cat

Funding information
Departament d'Universitats i Recerca; European Social Funds, Grant/Award Numbers: 2022 FI_B 00198, 2023 FI-2 00198; Banc de Sang i Teixits, Grant/Award Number: 2019.006.R; Instituto de Salud Carlos III (ISCIII), Grant/Award Number: 2021-SGR-00877

Abstract

Cell therapies based on multipotent mesenchymal stromal cells (MSCs) are traditionally produced using 2D culture systems and platelet lysate- or serum-containing media (SCM). Although cost-effective for single-dose autologous treatments, this approach is not suitable for larger scale manufacturing (e.g., multiple-dose autologous or allogeneic therapies with banked MSCs); automated, scalable and Good Manufacturing Practices (GMP)-compliant platforms are urgently needed. The feasibility of transitioning was evaluated from an established Wharton's jelly MSCs (WJ-MSCs) 2D production strategy to a new one with stirred-tank bioreactors (STRs). Experimental conditions included four GMP-compliant xeno- and serum-free media (XSFM) screened in 2D conditions and two GMP-grade microcarriers assessed in 0.25 L-STRs using SCM. From the screening, a XSFM was selected and compared against SCM using the best-performing microcarrier. It was observed that SCM outperformed the 2D-selected medium in STRs, reinforcing the importance of 2D-to-3D transition studies before translation into clinical production settings. It was also found that attachment efficiency and microcarrier colonization were essential to attain higher fold expansions, and were therefore defined as critical process parameters. Nevertheless, WJ-MSCs were readily expanded in STRs with both media, preserving critical quality attributes in terms of identity, viability and differentiation potency, and yielding up to 1.47×10^9 cells in a real-scale 2.4-L batch.

KEYWORDS
critical process parameters, GMP-compliant scale-up, human Wharton's jelly-derived mesenchymal stromal cells, microcarriers, stirred-tank bioreactors, xeno- and serum-free media

Abbreviations: 2D, two-dimensional; 3D, three-dimensional; ATMP, advanced therapy medicinal product; CPD, cumulative population doublings; CPP, critical process parameter; CQA, critical quality attribute; DMEM, Dulbecco's Modified Eagle Medium; DO, dissolved oxygen; DPBS, Dulbecco's Phosphate-Buffered Saline; EA, enhanced attachment; GMP, good manufacturing practices; hPL, human platelet lysate; HSA, human serum albumin; hSerB, human serum B; M, micelle; MC, microcarrier; MCB, master cell bank; MSC, mesenchymal stromal cell; PAT, process analytical technology; QbC, quality by control; QbD, quality by design; SA-β-Gal, senescence associated-β-galactosidase; SCM, serum-containing medium; STR, stirred-tank (bio)reactor; VCD, viable cell density; WJ-MSC, Wharton's jelly-derived mesenchymal stromal cell; XSFM, xeno- and serum-free medium.

Alba López-Fernández and Víctor Garcia-Gragera contributed equally to this work.

1 | INTRODUCTION

Advanced therapy medicinal products (ATMP) are revolutionizing the field of regenerative medicine due to their success in treating the root cause of diseases and unmet medical needs by augmenting, repairing, replacing, or regenerating organs, tissues, cells, genes and metabolic processes in the body. Accordingly, there is a growing demand for substances of human origin and the products of their manipulation in order to conduct late phase II/III clinical trials and meet commercial scale requirements.[1,2]

Human multipotent mesenchymal stromal cells (MSCs) derived from umbilical cord Wharton's jelly (WJ-MSCs) are emerging as an attractive starting material for the generation of allogeneic, banked, off-the-shelf MSC-based ATMP for use in different indications such as immune disorders and regenerative medicine,[3,4] and more recently, in severe COVID-19 patients.[5] Advantages over other tissue sources such as bone marrow or adipose tissue include (i) the use of non-invasive procedures for tissue extraction; (ii) greater proliferative potential; and (iii) higher immunomodulatory properties.[6] Clinical-grade Good Manufacturing Practice (GMP)-compliant MSCs are typically manufactured using 2D systems, media supplemented with either animal-derived components or human platelet-lysate (hPL) or serum, and yielding single or multiple doses in the range of 10^6–10^7 cells kg^{-1} body weight.[4,7] Some works have even considered resembling in vivo structures with the use of 3D scaffolds.[8] However, increasing cell number and diversification of clinical indications from a limited tissue source requires a paradigm shift in manufacturing platforms, from 2D to scalable and automated 3D strategies that offer standardized, robust, fully monitored and reproducible cell production platforms in compliance with current GMP.[9] Alternatives such as cell factories (e.g., HYPERStacks from Corning or Xpansion multiplate bioreactor from Pall) allow an increase in available cell culture surface but may only offer intermediate solutions when compared to 3D systems. Cell culture bioprocessing strategies such as hollow fiber bioreactors (e.g., Quantum Cell Expansion System from Terumo)[10] and microcarriers (MCs), together with vertical wheel bioreactors,[11–13] wave bioreactors[14] and stirred-tank (bio)reactors (STRs), provide an increased surface-to-volume ratio in cultures requiring large area attachment surfaces, thus contributing to cost-efficient process designs. Among them, spinner flasks and STRs have been widely investigated,[15–24] since they are versatile systems and easy to scale up. However, their use in a clinical-grade manufacturing process must comply with the corresponding regulations, which usually go hand in hand with each region's legislation (e.g., Directive 2003/94/EC and Directive (EU) 2017/1572) and quality guidelines (e.g., ICH Q5A, Q6B, Q7A, Q8, Q9, Q10, and Q11). From a process development perspective, critical quality attributes (CQAs) need to be defined as soon as possible in order to identify which critical process parameters (CPPs) have the highest impact on the final medicinal product. Implementing process analytical technologies (PATs) also aids in designing an operational space following quality by design (QbD) principles or, together with precise control methods, the more recent concept of quality by control (QbC).[25] Consequently, xeno- and serum-free materials (i.e., media, microcarriers, dissociation reagents) are preferentially used to reduce the risk of zoonotic contamination, reduce batch-to-batch variability and simplify the bioprocess.[23] Serum-free media has generally been reported to support higher cell expansion efficiencies compared to serum-containing media (SCM) in 2D cultures.[26] However, serum-free formulations developed for 2D cultures may lack the protective hydrodynamic effect associated with serum[27] and compromise initial cell attachment to microcarriers, thus affecting later cell growth. Seeding therefore requires optimization when transitioning from 2D to microcarrier-based cultures, considering options such as refinements to the medium composition and microcarrier coating.[28,29] The majority of studies conducted to date refer to large-scale expansion of MSCs from bone marrow and adipose tissue sources,[30] and only a few have reported the expansion of WJ-MSCs on microcarriers in spinner flasks[17,18,22,31–33] or STRs[17,18,20,31,34] using different experimental approaches based mainly on the use of hPL and SCM.

Herein, we report the development of a fully scalable GMP-compatible bioprocess based on the use of microcarriers for clinical grade production of WJ-MSCs. To this end, we tested four commercially available xeno- and serum-free media (XSFM) as an alternative to SCM for WJ-MSC expansion in 2D cultures. Two different GMP-compliant microcarriers were compared in a pilot approach toward STR expansions. The microcarrier that yielded better results was subsequently used to evaluate XSFM and SCM performances in an improved STR protocol, preserving the identity and multipotency of WJ-MSCs in a dynamic 3D environment. Our approach allowed us to identify the main CPPs and to implement continuous monitoring and parameter control, key for later QbD or QbC strategies implementation.

2 | MATERIALS AND METHODS

2.1 | WJ-MSC 2D culture in xeno-free, serum-free media, and serum-containing media

WJ-MSCs were sourced from a master cell bank (MCB) stored in a liquid nitrogen tank for long-term storage, as reported elsewhere.[35] Cryovials of WJ-MSCs with approximately 15 cumulative population doublings (CPD) were thawed and cultured in four commercial XSFM, namely PRIME-XV MSC Expansion XSFM (Fujifilm Irvine Scientific); MSC Nutristem XF (Biological Industries); MesenCult–ACF Plus Medium (StemCell Technologies); and MSC-Brew GMP Medium (Miltenyi Biotec). They were then further compared to 2D-SCM, consisting of low-glucose (1 g L^{-1}), 4 mM L-glutamine, Dulbecco's Modified Eagle Medium (DMEM, Gibco, Life Technologies) supplemented with 10% human serum B (hSerB, *Banc de Sang i Teixits*). Briefly, cells were plated at a cell density of 2×10^3–3×10^3 cells cm^{-2} in uncoated standard culture flasks (SPL Life Sciences) and maintained at 37°C in a humidified atmosphere of 95% air and 5% CO_2. XSFM and 2D-SCM were renewed every 3–4 days. At confluence, cells were washed with Dulbecco's Phosphate-Buffered Saline (DPBS, Lonza) and harvested using 0.05% trypsin-EDTA (Gibco) for 2D-SCM cultures, while 1x TrypLE Select CTS

(Gibco) was used for XSFM cultures. WJ-MSCs were expanded in each medium up to passage 6 to study their identity, differentiation potency, and kinetic parameters.

2.2 | WJ-MSC culture on microcarriers in a stirred-tank bioreactor

In a pilot protocol, two xeno-free microcarriers (Micelle microcarriers [M-MC], Aglaris Ltd Group; and Corning Enhanced Attachment microcarriers [EA-MC], Corning) were used following a pilot protocol for the expansion of WJ-MSCs in a STR using MSC-Brew GMP Media (XSFM) or 3D-SCM, consisting of high-glucose (4.5 g L^{-1}), GlutaMAX (3.97 mM), DMEM (Gibco, Life Technologies) supplemented with 10% (v/v) hSerB as control 3D medium. A benchtop 0.25-L STR (MiniBio, Applikon Biotechnologies) equipped with a down-pumping marine impeller (three-blade 45° pitched, diameter (D_i) = 22 mm) and temperature, pH and dissolved oxygen (DO) sensors, was used with an in-house closed-system configuration. Cryopreserved WJ-MSCs from passages 2–3 after MCB establishment (estimated CPD = 20–25) were thawed, conditioned with XSFM or 3D-SCM and seeded at a cell density of 5×10^3 cells cm^{-2} onto either 1000 cm^2 of M-MCs (17.5 g L^{-1}; 285 cm^2 g^{-1}; ρ_p = 1066 g mL^{-1}) or EA-MCs (13.9 g L^{-1}; 360 cm^2 g^{-1}; ρ_p = 1026 g mL^{-1}). Each microcarrier was prepared according to the manufacturer's instructions. DO was maintained at 70% by headspace flushing with air, pH was adjusted to 7.4 and controlled by CO_2 headspace injection, and temperature was controlled via heating blanket at 37°C. Cell adhesion was promoted for 4 h under intermittent agitation cycles (40'' stirring at 100 rpm and 30′ at 0 rpm) using a working volume of 50 mL. Next, continuous agitation was set at 110 rpm and the working volume adjusted to 200 mL, with a liquid height/vessel diameter ratio (H/D_i) of 1.56. Agitation was gradually increased from day 1 until it reached 140 rpm at the end of the culture after 6 days. At day 4, 50% (v/v) media were exchanged (with an additional 50% (v/v) media exchange at day 5 for the XSFM condition). Briefly, stirring was stopped for microcarrier sedimentation and 100 mL of spent media were removed and renewed with fresh XSFM or 3D-SCM. A 1.5-mL sample was collected twice a day for cell number and viability counting, cell morphology and microcarrier colonization assessment, and determination of nutrient/metabolite concentration.

In an improved protocol, variations were applied to the pilot protocol. The total vessel volume was adjusted to 130 mL in order to reduce the H/D_i to 1 and an additional three-blade impeller was included (spacing to diameter ratio (S/D_i) = 2). Because of volume adjustment, the EA-MC concentration was increased to 21.38 g L^{-1}, preserving 1000 cm^2 of microcarrier surface. Before sample extraction (once or twice daily), agitation was adjusted according to Zwietering's equation[36] (Equation 1) and the kinematic to dynamic viscosity relation (υ; in m^2 s^{-1}) (Equation 2) to ensure proper microcarrier distribution throughout the vessel for representative sample collection. This speed was maintained for 40 s before sample extraction and returned to its previous value after sampling.

$$N_{js} = Sv^{0.1} d_p^{0.2} \left(g \frac{\rho_p - \rho_m}{\rho_m} \right)^{0.45} B^{0.13} D_i^{-0.85} \quad (1)$$

$$v = \frac{\eta}{\rho_m} \quad (2)$$

N_{js} refers to minimum speed for particle suspension [s^{-1}]; S, dimensionless parameter dependent on impeller and tank geometry; d_p, particle diameter [m]; g, gravity acceleration (9.81 m^2 s^{-1}); ρ_p, particle density [kg m^{-3}]; ρ_m, medium density [kg m^{-3}], B; solid-to-liquid mass ratio [%], D_i, impeller diameter [m]; and η, medium dynamic viscosity [Pa s].

2.3 | Stirred-tank bioreactor harvesting protocol

At day 6, agitation was stopped, microcarriers were allowed to settle and supernatant was removed. Attached cells were washed with DPBS and 30 mL of either 0.25% trypsin-EDTA (Gibco), in the case of SCM cultures, or TrypLE 10x (Gibco) in the case of XSFM cultures, were added to the vessel. Enzymatic cell detachment was performed under agitation at 150 rpm and 37°C for 3′. In all cases, the enzymatic reaction was quenched by adding 50 mL of saline solution (Plasmalyte 148, Baxter) supplemented with 10% (w/v) human serum albumin (HSA, Grifols). Cell suspensions were separated from microcarriers using a filtration bag (Miltenyi Biotec) with two meshes of decreasing pore sizes of 175 and 40 µm, respectively. Cells were centrifuged at 340 × *g* for 10′, re-suspended in either 3D-SCM or XSFM, and subsequently cryopreserved for further characterization.

2.4 | Cell number and viability assessment

Viable and total cell number were determined by the hemocytometer-based Trypan blue (GE Healthcare) dye exclusion assay. This information was used to calculate the viable cell density (**VCD**) [cell cm^{-2}], **cell viability** [%], **CPD**, **fold expansion**, observed growth rate (μ_{obs}), average growth rate (μ_{avg}), and average cell productivity (V_P). These parameters were calculated according to Equations (3–9), respectively, where CPD_0 refers to the initial CPD, **A** to the culture surface used, X_t to the number of viable cells at a given time, X_{TOTt} to the number of total cells at a given time, X to the final number of viable cells, X_0 to the number of seeded viable cells, X_{att} to the number of attached viable cells on microcarriers at day 1, t to the culture time and **V** to total volume of media consumed for each expansion. Maximal growth rate (μm_{ax}) was calculated analogously to μ_{avg} but using only exponential growth phase values and applying linear regression.

$$VCD_t = \frac{X_t}{A} \quad (3)$$

$$Viability_t = \frac{X_t}{X_{TOT_t}} \ [\%] \quad (4)$$

$$CPD = CPD_0 + \frac{\ln \frac{X}{X_0}}{\ln 2} \quad (5)$$

$$fold\ expansion = \frac{X}{X_0} \quad (6)$$

$$\mu_{obs} = \frac{\ln \frac{X}{X_0}}{t} \quad (7)$$

$$\mu_{avg} = \frac{\ln \frac{X}{X_{att}}}{t} \quad (8)$$

$$V_P = \frac{X - X_0}{t \cdot V} \quad (9)$$

2.5 | Cell attachment assessment

Live/Dead cell viability assay (Life Technologies) and fluorescent nuclear staining (Hoechst 33342, Life Technologies) were performed to assess cell attachment, distribution, morphology and viability. After staining, images were captured using an inverted fluorescence microscope (Leica DFC450, Leica DMIL LED; Leica Microsystems).

The number of cells per microcarrier was manually counted from Live/Dead fluorescent images (number of microcarriers analyzed per time point ≥320) using ImageJ2 Software (see 2.3.0/1.53q, National Institutes of Health, USA). The percentage of microcarrier colonization was calculated as the number of microcarriers with at least one living cell attached; WJ-MSC attachment efficiency on microcarriers was also calculated (ratio of adhered cell number/theoretical average cell number per microcarrier). The theoretical average cell number adhered after 24 h was calculated based on the number of cells seeded, the total surface available and the average surface per microcarrier (Equation 10). To calculate the average surface per microcarrier, microcarrier diameters at each time point were also measured using ImageJ2.

$$\frac{theoretical\ average\ cell\ number}{microcarrier} = \frac{surface}{microcarrier} \cdot \frac{total\ seeded\ cells}{total\ surface\ available} \quad (10)$$

2.6 | Metabolism analysis

Nutrients and metabolites from supernatants collected daily were measured using automatic analyzers for glucose and lactate concentration (Y15, Biosystems S.A.) and glutamine and glutamate concentration (YSI 2950D, Xylem Incorporated).

Specific glucose consumption (q_{Glc}) and specific lactate production (q_{Lac}) rates were calculated for each medium replacement (culture days 0–4, days 4–5, and days 5–6) analogously to previous works.[37] For each growth period, regression of the glucose or lactate concentration [(g glucose or g lactate) mL^{-1}] versus the Integral of Viable Cell Concentration (IVCC) [$\times 10^9$ cells day mL^{-1}] was performed. Biomass to glucose ($Y_{X/Glc}$) and biomass to lactate ($Y_{X/Lac}$) yields were calculated as a regression of glucose or lactate concentration versus the Viable Cell Concentration (VCC) [$\times 10^9$ cells day mL^{-1}] to improve data reliability and precision. Lactate to glucose ($Y_{Lac/Glc}$) yields were also calculated as a regression of the lactate to glucose concentration for each phase.

2.7 | Immunophenotype assessment

Immunophenotypic characterization of WJ-MSCs from XSFM and SCM cultures in 2D were performed using the following antibodies: CD45-FITC (Clone HI30), CD73-PE (Clone AD2), CD31-FITC (Clone WM59) (BD Pharmingen), CD105-PE (Clone 43A4E1; Miltenyi Biotec), HLA-DR-FITC (Clone L243; BD Biosciences), and CD90-PE (Clone F15-42-1-5; Beckman Coulter). XSFM and SCM cultures in 3D were performed using the following antibodies: CD45-APC-AlexaFluor750 (Clone J33), CD73-PE (Clone AD-2), CD31-Pacific Blue (Clone 5.6E), HLA-DR-APC (Clone Immu-357), and CD90-FITC (Clone F15-42-1-5) (all from Beckman Coulter) and CD105-PE-Vio 770 (Clone REA794; from Miltenyi Biotec). In all cases, cell suspensions at a concentration of 1×10^6 cells mL^{-1} were stained for 15′ at room temperature, washed and re-suspended in DPBS, as described elsewhere.[38] Acquisition and data analysis were performed using a FACSCalibur cytometer and CellQuest Pro software (Becton Dickinson), respectively, in 2D cultures, and a Navios EX device and Navios EX software (version 2.0, Beckman Coulter), respectively, in 3D cultures.

2.8 | Differentiation assays

WJ-MSCs from XSFM and SCM cultures were seeded at a cell density of 1×10^4 cells cm^{-2} in 24-well plates for adipogenic and osteogenic differentiation or seeded in 5 µL micromasses at 1.6×10^7 cells mL^{-1} in 24-well non-adherent plates for chondrogenic differentiation, in expansion medium. Between 2 and 24 h after seeding, specific differentiation medium formulations (StemPro; Gibco) supplemented with 100 unit mL^{-1} of penicillin and 100 µg mL^{-1} of streptomycin (Sigma-Aldrich) were used for in vitro adipogenic, chondrogenic, and osteogenic induction of WJ-MSCs. On day 35 after differentiation induction, Oil Red O (Sigma-Aldrich), Safranin O (Sigma-Aldrich), and Alizarin Red (Merck Millipore) staining were performed to assess qualitatively the differentiation, and images were captured using an inverted microscope (Leica DFC450, Leica DMIL LED).

2.9 | Senescence assay

Senescence associated-β-galactosidase (SA-β-Gal) activity was measured using a Cellular Senescence Assay Kit (Merck Millipore). At least 1×10^6 cryopreserved cells from the improved protocol harvests were thawed and seeded in triplicate at 2×10^4 cells cm^{-2} in 6-well plates and further incubated for 24 h at 37°C in a humidified atmosphere of 95% air and 5% CO_2 assay conditions. Additional triplicate sets were

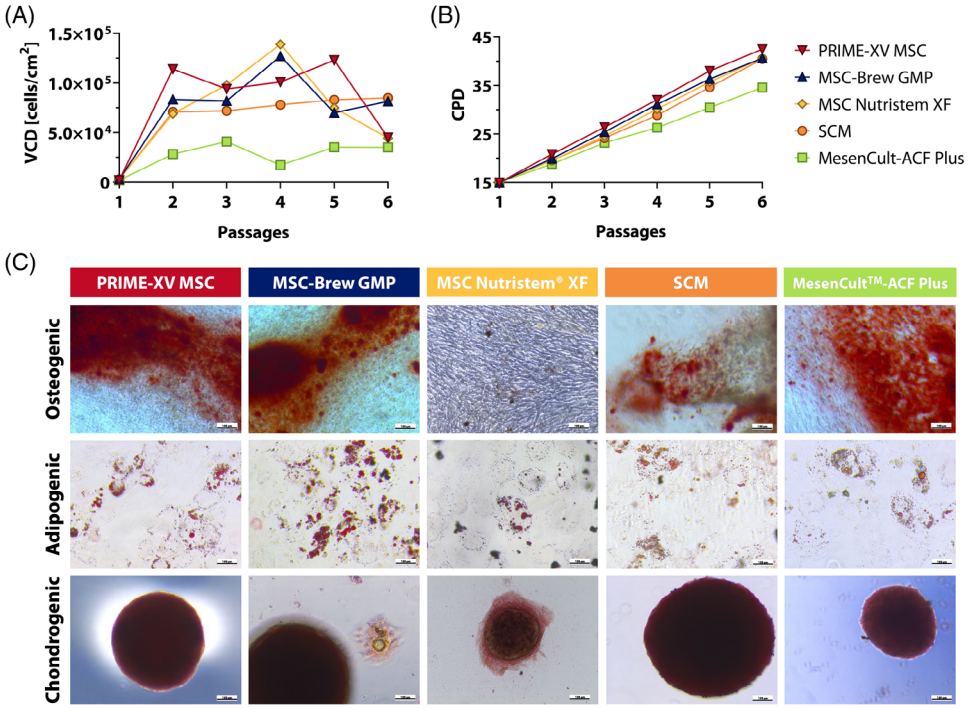

FIGURE 1 Xeno-/serum-free media (XSFM) screening and comparison with the serum-containing medium (SCM) of reference on 2D expansions. (A) Viable cell density (VCD) per passage. (B) Cumulative population doublings (CPD) per passage. (C) Representative images of multilineage in vitro differentiation potential of WJ-MSCs cultured in different commercial XSFM and SCM (passage = 6) upon induction into osteogenic (Alizarin Red staining), adipogenic (Oil Red O staining) and chondrogenic (Safranin O staining) lineages after 35 days (scale bar 100 μm). Subfigures (A) and (B) share legend.

seeded to calculate the total cell number after 24 h. WJ-MSCs were stained following the manufacturer's instructions and positive cells were counted to calculate the percentage of senescent cells.

2.10 | Data analysis

Data collection and analysis were performed with Microsoft Excel (Microsoft Corp). GraphPad Prism (v5.03, GraphPad Software, Inc.) was used for statistical analysis and graphics. Results are presented as mean ± standard deviation. Unpaired Student's *t*-tests were conducted for group comparisons, applying Welch's correction when needed. Statistical significance was set at p-value <0.05 (*). Other degrees of significance are also indicated (**p-value <0.01; ***p-value <0.001; ****p-value <0.0001).

3 | RESULTS

3.1 | WJ-MSC culture in xeno-/serum-free and serum-containing media

Cells were successfully thawed and expanded in four commercial XSFM using SCM as comparison. When compared to SCM, harvested VCD and CPD were higher in early passages for three out of four XSFM, while they decreased in late culture passages in XSFM conditions (Figure 1A,B). These observations were supported by higher average fold expansion per passage, with PRIME-XV MSC Expansion XSFM showing the best average value (47.7 ± 15.1), followed by MSC-Brew GMP Medium (29.6 ± 7.3), MSC Nutristem XF (28.4 ± 11.9), SCM (25.9 ± 2.1), and lastly, MesenCult-ACF Plus (15.7 ± 4.5). The μm_{ax} was also illustrative of this difference in performance (MSC-Brew GMP Medium = 0.90 ± 0.03 day^{-1} and SCM = 0.63 ± 0.01 day^{-1}).

Spindle-shaped morphology was preserved upon passaging of undifferentiated WJ-MSCs in both XSFM and SCM. Osteogenic, adipogenic, and chondrogenic lineage commitment was confirmed (Figure 1C). In all conditions, immunophenotypic analysis was consistent with mesenchymal identity, being positive for CD73/CD90/CD105 and negative for CD31/CD45/HLA-DR both at passages 1 and 6.

Based on these results, because of its culture performance and consistency throughout passages in terms of fold expansion, multipotency and identity preservation, PRIME-XV MSC Expansion XSFM should be considered as the best option. MSC Brew GMP Medium would be the first runner-up regarding fold expansion and with qualitatively better adipogenic differentiation. Nevertheless, knowing that the intention of this work was an efficient transition from 2D productions to GMP-compatible ones in stirred-tank bioreactors, having at hand a medium manufactured under cGMP conditions was a strong requirement. Although both these two media comply with this certification, only MSC-Brew GMP is formulated in a closed bag system. It was considered worth sacrificing the quantitative outcome of the bioprocess in favor of a medium which would allow for a closed-system

TABLE 1 Main metrics for Wharton's jelly-derived mesenchymal stromal cell expansions in stirred-tank bioreactor.

	Microcarrier		Medium		Harvested VCD	Total CPD	Fold expansion	μ_{obs}	μ_{avg}
n	Type	Conc. [g L^{-1}]	Type	V [mL]	[cell cm^{-2}]			[day^{-1}]	[day^{-1}]
Metrics with the pilot protocol for microcarrier screening									
1	M	17.5	SCM	200	3.0×10^4	27.2	5.9	0.37[a]	0.53[a]
1	EA	13.9	SCM	200	4.8×10^4	27.9	9.5	0.44[a]	0.48[a]
Metrics with the improved protocol for media screening									
3	EA	21.4	XSFM	130	$3.2 \times 10^4 \pm 5.6 \times 10^3$	25.8 ± 0.5	6.4 ± 1.1	0.37 ± 0.03	0.51 ± 0.03
3	EA	21.4	SCM	130	$6.7 \times 10^4 \pm 1.3 \times 10^3$	26.8 ± 2.8	13.4 ± 2.5	0.50 ± 0.04	0.54 ± 0.04

[a]Pilot protocol μ_{obs} and μ_{avg} values were calculated using an estimated VCD before harvest based on the harvested VCD and assuming the same harvest yield from optimized protocol batches. Conc., concentration; V, volume.

bioprocess, which ultimately would result in a more successful translation and validation of the developed bioprocess for advanced therapies. Consequently, MSC-Brew GMP Medium was selected for further use.

3.2 | Pilot protocol for WJ-MSC culture on microcarriers in a stirred-tank bioreactor

Two independent experiments were performed in the STR to evaluate a pilot protocol for WJ-MSC expansion using SCM and two different GMP-compliant microcarriers (namely EA-MCs and M-MCs). Harvested VCD, CPD, fold expansion, μ_{obs}, and μ_{avg} are shown in Table 1, revealing superior results in harvested VCD, fold expansion and μ_{obs} with EA-MCs. V_P and colonization were also higher with EA-MCs (Figure 2A,C), whereas harvest yield percentage was similar using both MCs (Figure 2B). Regarding colonization efficiency on EA-MCs, an efficiency of 80.76% was obtained at 24 h after seeding (day 1), reaching a maximum of 99.59% at day 6. However, colonization efficiency using M-MCs was only 36.62% at day 1, reaching a maximum colonization of 78.98% (Figure 2C). Based on these results, EA-MCs were chosen for developing a GMP-compliant bioprocess for WJ-MSC expansion in STR.

3.3 | Protocol improvement and best media comparison for WJ-MSC culture on microcarriers

Experiments were performed in triplicate to improve the pilot protocol, using EA-MCs with both SCM and XSFM. Using Zwietering's equation, the exact values for ensuring suspension of solids were calculated as 182.23 rpm for SCM ($\rho_m = 1009$ kg m^{-3} and $\eta = 9.3 \times 10^{-4}$ Pa s)[39] and 194.70 rpm for XSFM (assuming the MSC-Brew GMP Medium had similar properties to other XSFM such as mTeSR™1, $\varrho_m = 1006$ kg m^{-3} and $\eta = 8.5 \times 10^{-4}$ Pa s),[40] applying the configuration ($B = 2.12\%$, $D_i = 22$ mm, $d_p = 168.5$ µm, and $\rho_p = 1026$ g mL^{-1}). S was assumed to be 10 in accordance with similar configurations and considering the negative effect of pieces near the bottom (e.g., sparger).[41] Based on this calculation, the adjusted speed before sample extraction was rounded up to 200 rpm. Harvested VCD, CPD, fold expansion, μ_{obs}, and μ_{avg} are summarized in Table 1.

Under these conditions, WJ-MSC expansion in SCM showed significantly higher cell densities, fold expansions, μ_{obs} and V_P (Figure 2A) than in XSFM, while CPD, μ_{avg} and harvest yields were similar (Figure 2B). Moreover, these yields from the improved protocol (67.64 ± 9.03% and 65.02 ± 4.97%) were higher than the apparent yields obtained from the pilot protocol experiments (40.35% and 36.14%).

The percentage of microcarrier colonization was significantly higher in SCM (79.95 ± 5.68%) when compared to XSFM (45.07 ± 7.55%) at 24 h after seeding and was still significantly higher at day 6: 98.86 ± 1.10% and 91.36 ± 7.03%, respectively (Figure 2C). Microcarrier aggregates were visible from day 4 onwards and increased in size throughout the culture time in all cases, while the number of dead cells directly observed was negligible. Empty microcarriers were visible throughout the culture time, but in a higher proportion with XSFM cultures, together with a reduced attachment efficiency (20.29 ± 5.81% vs. 53.14 ± 15.10% in SCM) (Figure 2D,E). The maximum attainable adherent cells per microcarrier (assuming a Poisson distribution mean value (λ) equal to the theoretical average cell number per microcarrier) was compared to the distributions actually obtained, being more similar in SCM expansions (Figure 2F). Higher harvested VCDs were obtained in batches with higher attachment efficiencies and microcarrier colonization percentages at day 1, as observed in all SCM culture experiments (Figure 2G,H). This trend was more illustrative in the case of microcarrier colonization ($R^2 = 0.834$) than in attachment efficiency ($R^2 = 0.634$).

3.4 | Cell growth profile and metabolism

Glucose concentration differed between SCM and XSFM, being higher in SCM for the whole culture. XSFM presented a lower initial glucose concentration (≥0.12 ± 0.11 g L^{-1}) before medium changes and before cell harvesting (Figure 3A). Initial glutamine concentration profiles were similar for both media, but differed throughout the culture time, again showing faster consumption rates in SCM (Figure 3B). Maximum lactate concentration values measured were 1.63 ± 0.14 g L^{-1} for

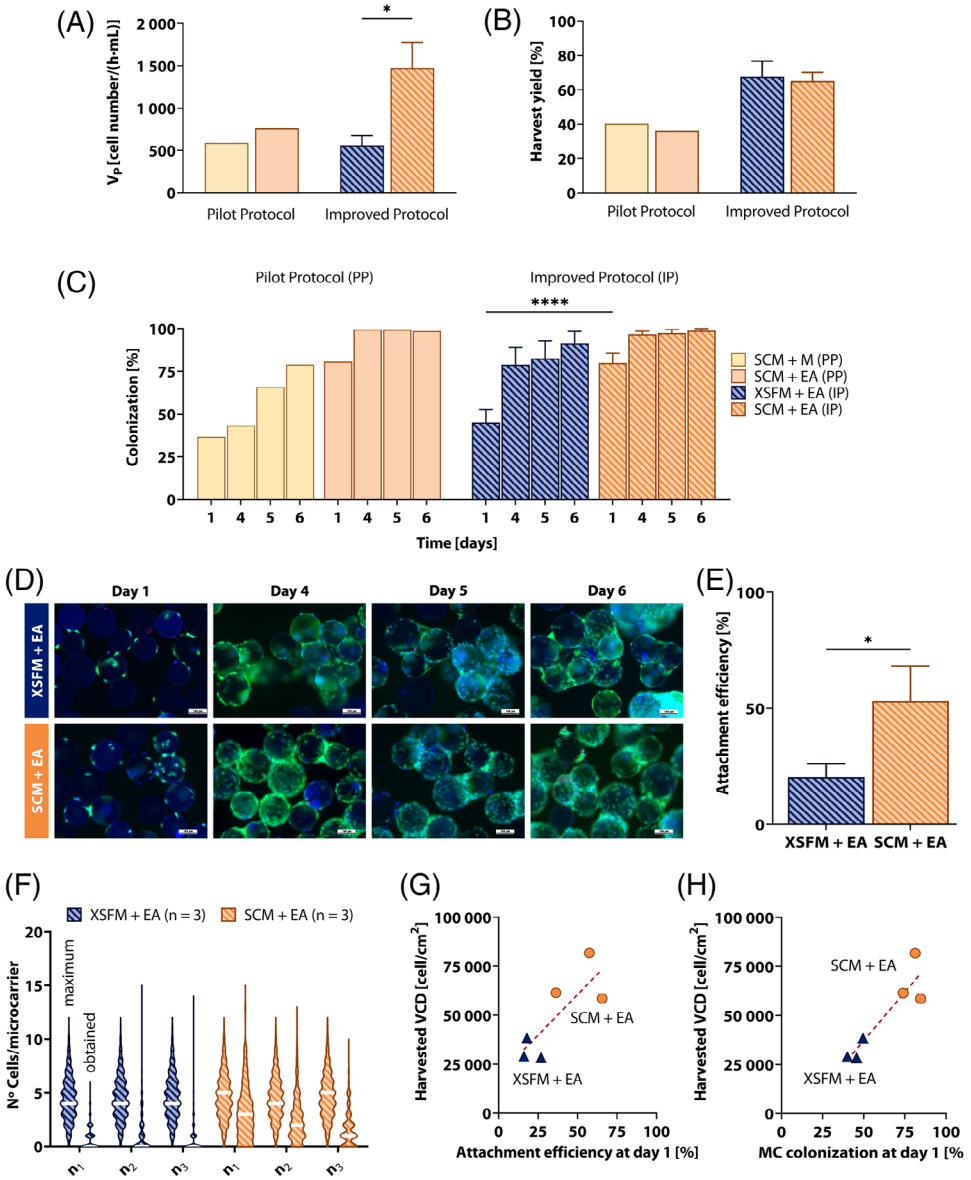

FIGURE 2 Bioprocess assessment of pilot and improved protocols. (A) Average cell productivity (VP), as cell number obtained per hour of culture and mL of medium consumed. (B) Percentage of harvest yield. (C) Percentage of colonization throughout the cultures. For clarity, statistical test is only shown between colonization values at day 1, but significance was maintained over days 4 (***), 5 (***), and 6 (**). (D) Representative images of WJ-MSCs from SCM and XSFM cultures on EA-MCs after Live (green)/Dead (red) and Hoechst (blue) staining on different culture days (scale bars 100 μm). (E) Attachment efficiency of the improved protocol experiments. (F) Attachment efficiency on microcarriers in detail. The distribution on each of the optimized protocol experiments at day 1 of culture is shown. Side-by-side comparison of maximum number of attainable and obtained adherent cells per microcarrier. White lines indicate distribution medians. (G) Harvested VCD regression on the attachment efficiency at day 1 ($R^2 = 0.647$) and (H) on the microcarrier colonization at day 1 ($R^2 = 0.834$). Subfigures (A), (B), and (C) share legend. Plain bars and striped bars refer to the pilot ($n = 1$, each condition) and improved protocol ($n = 3$, each condition) respectively. Light yellow (■), blue (▲), and orange (●) indicate SCM + M, XSFM + EA, and SCM + EA conditions, respectively.

SCM and 0.98 ± 0.17 g L^{-1} for XSFM cultures (Figure 3C) in accordance with glucose consumption, and maximum glutamate concentrations were 0.080 g L^{-1} for SCM and 0.104 g L^{-1} for XSFM cultures (Figure 3D). VCDs were higher in SCM cultures than in XSFM cultures in all measurements performed, having a maximum cell density of $1.05 \times 10^5 \pm 2.72 \times 10^4$ cells cm^{-2} versus $5.00 \times 10^4 \pm 1.76 \times 10^4$ cells cm^{-2} before cell harvesting in SCM and XSFM, respectively. Additionally, harvested VCD was significantly higher in SCM than in XSFM cultures ($6.72 \times 10^4 \pm 1.26 \times 10^4$ cells cm^{-2} vs. $3.18 \times 10^4 \pm 5.58 \times 10^3$ cells cm^{-2}; p-value <0.05) (Figure 3E).

Regarding biomass yields, biomass to glucose ($Y_{X/Glc}$) and biomass to lactate ($Y_{X/Lac}$) in XSFM (0.15 ± 0.11 and $0.13 \pm 0.09 \times 10^9$ cells g^{-1}, respectively) were 0.44 and 0.52 times the SCM yields. Higher apparent q_{Glc} and q_{Lac} values were obtained in XSFM cultures (3.16 ± 0.61 and 3.33 ± 0.56 g/(10^9 cells·day), respectively) compared to SCM cultures (1.51 ± 0.58 and 1.89 ± 0.39 g/(10^9 cells day)) (Figure 3F).

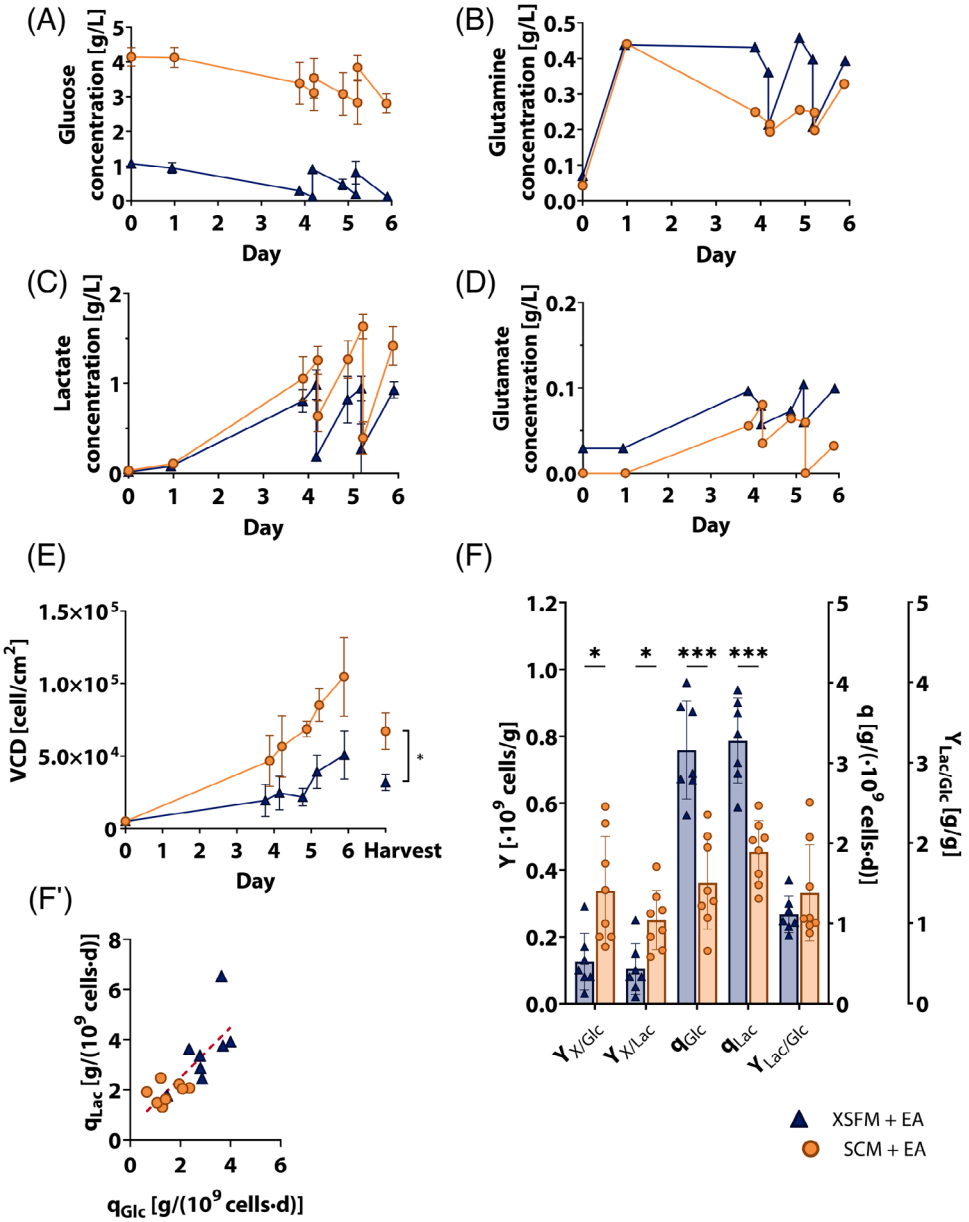

FIGURE 3 Metabolic analyses of the improved protocol experiments. Nutrient and metabolite concentration profiles for (A) glucose, (B) glutamine, (C) lactate, and (D) glutamate. (E) VCD profile and harvested VCD. Values are shown as mean ± standard deviation ($n = 3$). (F) $Y_{X/Glc}$. $Y_{X/Lac}$, $Y_{Lac/Glc}$, $q_{Glc, qLac}$, and $Y_{Lac/Glc}$ values obtained from each media change for the XSFM + EA versus SCM + EA triplicates, considering each medium change as separate growth ($n = 7$ and $n = 8$, respectively). (F') q_{Lac} regression on the q_{Glc} ($R^2 = 0.599$). (▲) represents XSFM + EA batches and (●), SCM + EA batches. Statistical tests shown in subfigures (E) and (F) for better clarity.

Notably, low q_{Lac} values linearly correlated with lower q_{Glc} values, as shown in Figure 3F'. In contrast, lactate to glucose yields showed similar values in both conditions ($Y_{Lac/Glc} = 1.11 \pm 0.23$ g g^{-1} and $Y_{Lac/Glc} = 1.38 \pm 0.60$ g g^{-1}) (Figure 3F).

3.5 | CQA of stirred-tank bioreactor-expanded WJ-MSCs

WJ-MSCs resulting from both SCM and XSFM maintained high viabilities after harvest (≥92.07%; 95.90 ± 2.84%), and readily attached to plastic surfaces upon replating. The percentage of senescent cells was below 0.015% for all conditions (Figure 4A). Immunophenotypic results showed no significant differences between XSFM and SCM cultures in the MSC surface expression profile. However, CD105 expression was slightly lower in harvested cells from SCM cultures, due to the positivity of one of the triplicates reaching 88.39% (Figure 4B). Regarding multipotency, the osteogenic potential was confirmed by Alizarin Red staining of calcium deposits, adipogenic potential by Oil Red O staining of intracellular lipid droplets, and chondrogenic potential by Safranin O staining of proteoglycans (Figure 4C).

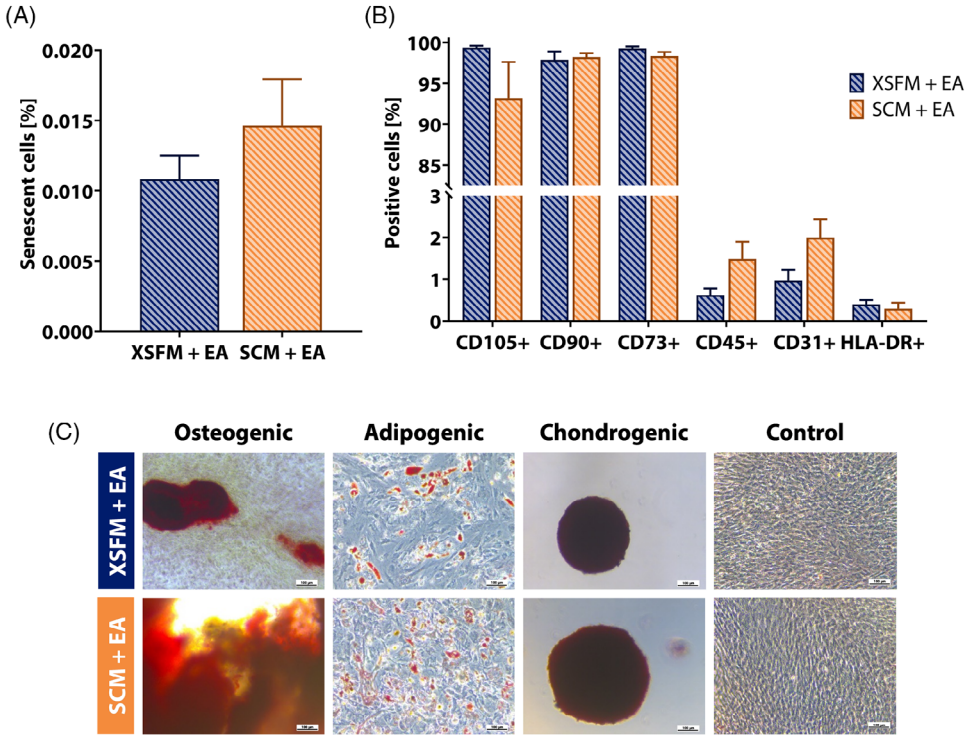

FIGURE 4 Characterization of Wharton's jelly-derived mesenchymal stromal cells (WJ-MSCs) after expansions in stirred-tank bioreactor (passage = 4–5) using the improved protocol under XSFM + EA ($n = 3$) and SCM + EA ($n = 3$) conditions. (A) Percentage of senescent cells. (B) Percentage of positive cells for the main positive (CD105, CD90, and CD73) and negative (CD45, CD31, and HLA-DR) immunophenotypic markers. (C) Representative images of multilineage in vitro differentiation potential upon induction into osteogenic (Alizarin Red staining), adipogenic (Oil Red O staining), and chondrogenic (Safranin O staining) lineages after 35 days (scale bar 100 μm). No statistical differences were found in any of the analyzed parameters.

4 | DISCUSSION

Large-scale MSC production under GMP regulations for the generation of ATMP is a manufacturing challenge, especially when transitioning from 2D to microcarrier culture under stirred conditions[42] and from serum-containing (and human platelet-containing) media to xeno-/serum-free media.[24] Balancing cost-effective production while preserving their CQA necessitate a thorough understanding of culture requirements, implementation of reliable on-line PATs, and either the incorporation of changes or optimizations into CPPs that may help to improve the efficiency of cell expansion.

Commercial XSFM represent a GMP-compliant alternative to conventional SCM, with additional benefits such as higher proliferation capacity and fold expansion while ensuring more homogeneous and reproducible bioprocessing.[26] However, each commercial alternative should be previously tested in order to introduce the most suitable option in each manufacturing process. We successfully demonstrated direct 2D-culture transition from SCM to XSFM in different commercially available alternatives, with WJ-MSCs retaining their necessary characteristics for potential therapeutic use. Additionally, average fold expansion was up to 1.84 times higher in XSFM cultures compared to SCM, showing an increased proliferative potential of XSFM that is consistent with other studies.[43,44]

Xeno-free, ready-to-use microcarriers prepared for working in closed systems can facilitate their introduction in GMP-compliant bioprocessing platforms.[45] Selection of the appropriate microcarrier based on cell type, bioprocessing criteria (seeding, proliferating and harvesting efficiency) and manufacturing requirements (e.g., GMP certificates) is essential in the pre-GMP development stage of scale-up protocols. In our case, we compared WJ-MSC adhesion and expansion onto two types of microcarriers: a commercially available ready-to-use microcarrier (EA-MC) and a customized microcarrier specifically designed for MSC expansion (M-MC) in a pilot protocol. To that end, small-scale 0.25-L STRs are suitable for media and microcarrier screening before proceeding with the manufacturing scale-up in fully GMP-compliant settings. Pilot protocol experiments resulted in a lower harvested VCD, probably related to poor homogeneity during culture. It is essential to maintain homogeneity in microcarrier cultures, since it allows the microcarrier surface usage to be maximized while avoiding local particle accumulation,[22,46] which in turn can lead to aggregation in high cell density conditions.[47] Specifically, in the pilot experiments, microcarriers accumulated and clustered below the impeller, where the lowest flow velocity occurs. This potentially led to overestimation of pre-harvest VCDs and, consequently, underestimation of harvest yields. In contrast, the improved protocol implemented variations based on observations from the pilot protocol, such as changes in the bioreactor geometry (H/D_i ratio), increased

stirring speed at sampling, frequent and larger volume media changes for XSFM cultures (to ensure nutrient supply under the new concentrated conditions) and a second pitched-blade impeller (chosen over other designs as the common one used in STRs for MSC expansion).[48] A significant increase in productivity was observed for the SCM batches in comparison to the previous SCM experiments performed following the pilot protocol. Importantly, under the improved protocol, reliable biomass monitoring was achieved, a key analytical tool, considering that one of the CQA may be the cell number yielded.

Improved protocol metrics were assessed in order to evaluate the effect of each medium in 3D cultures with GMP microcarriers, and to identify those CPP that could have a major impact on WJ-MSC production. Initial cell attachment onto the microcarriers was substantially lower in XSFM cultures, most likely due to a lack or reduced quantity of important cell adhesion-promoting proteins in commercial XSFM, such as fibronectin and vitronectin.[24] As suggested in the literature, the attachment of hMSCs on microcarriers can reach 70%–90% under the static or dynamic condition in SCM, whereas the efficiency significantly decreases to 22%–23% in XSFM.[14,24] Low attachment efficiencies on microcarrier inoculation can also result in a prolonged lag-phase at the beginning of the expansion process.[49] Nevertheless, there is also evidence that MSCs show increased proliferative potential and can achieve the same cell density in XSFM compared to SCM, despite the lower attachment efficiency.[15] In our study, SCM facilitated higher attachment efficiency and microcarrier colonization, allowing higher harvested VCD compared to XSFM. For this reason, these two parameters should be considered as CPP when evaluating culture performance, as they would further increase maximal cell density and productivity. This reinforces previous statements regarding the importance of a good initial attachment process.[15,28,45] The improved protocol showed two different colonization and final cell yield dynamics depending on whether SCM or XSFM was used. Further studies might consider using a cell-adhesion protein coating to improve low initial attachment[16] or other microcarrier composition that might increase or promote better cell attachment in combination with XSFM.[23]

In hMSC microcarrier culture, a long lag phase in cell proliferation is commonly observed,[19,24,49–52] suggesting that the cells need longer to adapt to the culture environment in bioreactors compared to 2D culture. The development of microcarrier culture systems for hMSC expansion is not yet fully mature, and may not have exploited the maximum expansion potential. hMSCs grow faster and show higher harvested VCD in 2D culture than in microcarrier culture, with higher proliferation rates and lower doubling times as reported herein, in line with the literature.[19,52] This was particularly notable in the XSFM used in our study, where the performance significantly shifted from MSC-Brew GMP Medium having a 1.43 times higher μm_{ax} than its SCM competitor in 2D to showing a μ_{obs} in 3D that was only 0.74 times the μ_{obs} obtained with SCM. This justifies the importance of identifying medium candidates in 2D, knowing that they may underperform in 3D and require optimization,[28] especially before translating the developed processes into clinical trials. This medium optimization step has already been reported to be a uniquely promising one since, when only the exponential phase is considered, microcarrier culture can display comparable or even increased growth rate after optimization.[52]

Currently, most studies on microcarriers only emphasize the attachment efficiency and expansion fold, but the recovery efficiency is equally critical for large-scale production.[48] Although the harvesting protocol in our study differed between SCM and XSFM in the detachment reagent used (trypsin 0.25%-EDTA vs. TrypLE 10x to ensure a complete xeno-free bioprocess in the XSFM cultures), this change in the enzymatic detachment process did not alter the efficiency in harvest yield, as the values obtained were similar in both conditions. Under both settings, our harvest yields showed similar or even higher values with respect to previous studies.[34,49,53] Moreover, the best harvested cell density obtained in these experiments, when translated into manufacturing scale STRs (2.4-L batch in a 3L-STR; 18000 cm^{2}[54]; 4.8 L medium consumed; 1.47×10^{9} cells), would be able to surpass even the highest harvested cell number reported to date from a hollow-fiber GMP-compliant system (standard-bioreactor; approx. 21000 cm^2; 5 L medium consumed; 6.05×10^{8} cells).[55]

Neither glucose nor glutamine limitation were observed in 3D improved protocol cultures, with lowest concentrations of 0.12 and 0.04 g L^{-1}, respectively. These values were higher than the reported Monod's half velocity constant in hybridoma (K_{Glc} = 0.02 g L^{-1}; K_{Gln} = 0.01 g L^{-1}).[56] Although glutamine was closer to being apparently limiting, its lowest concentrations were obtained with either fresh media or after partial medium changes, possibly because both SCM and XSFM may use glutamine-based dipeptides as more stable glutamine sources. Therefore, the profile observed corresponds to simultaneous alanyl-glutamine (SCM) or non-disclosed glutamine dipeptide (XSFM) hydrolysis by WJ-MSC extracellular peptidases[57] and their consumption. It is essential to measure biochemical parameters such as nutrient/metabolite concentration for these processes seeking to identify new CPPs and to develop tools to robustly predict and control the bioprocess outcome following QbC approaches. While glucose and glutamine are determining factors in cell culture metabolism and growth, lactate, glutamate and, if possible, ammonia concentrations should also be monitored in MSC cultures. High lactate levels above a certain threshold (3.19 g L^{-1}) inhibit MSC growth, and the glutamate profile is indicative of the amount of ammonia being produced, which is also inhibitory above 0.35 g L^{-1}.[58]

With respect to q_{Glc} and q_{Lac} values, these showed some correlation with one another, which may also help in developing simpler QbC designs (e.g., measuring consumption of only one of the metabolites to predict both). Moreover, these values are consistent with those reported in the literature, with XSFM ranging from 1.21 to 1.64 and 1.04 to 1.71[21,59] and SCM (and hPL-containing media) from 0.97 to 2.14 and 0.9 to 2.23 g/(10^{9} cells day), respectively.[17,19,23,33,50] Likewise, the μ_{obs} measured is similar or even a little higher than the ranges reported in previous studies for XSFM (0.36–0.54 day^{-1})[16,59] and SCM (0.41–0.52 day^{-1}),[17,50] and only some batches with immortalized MSCs showing slightly higher growth rates (0.65 day^{-1})[23] or using special hPL-based supplements (UtraGRO™; 1.00 day^{-1}) have been found.[16] Based on the reported data, there is no difference between XSFM and SCM consumption, production and growth rates,

demonstrating that the particular characteristics in each expansion process may contribute more to the observed variability than the type of medium per se. Nonetheless, in our study, the direct comparison between XSFM and SCM showed a clear difference in terms of higher biomass yields and growth rates and lower glucose consumption and lactate production rates in SCM. One hypothesis may be that SCM sustained growth with a wider variety of carbon sources than XSFM (e.g., glutamine as observed in the profile but also other amino acids and nutrients differentially found in DMEM and serum), which led to a higher apparent yield than the actual biomass produced per unit of glucose. On the other hand, $Y_{Lac/Glc}$ was slightly higher than 1 g g^{-1} for both conditions. Besides implying that aerobic glycolysis was predominant as a less energy-efficient but higher proliferation strategy, commonly known as the Warburg effect,[60] $Y_{Lac/Glc} \geq 1$ g g^{-1} (theoretical maximum) also infers that part of the glutamine was oxidated following glutaminolysis[61] and could generate more lactate as previously reported.[33,62,63] This may also be supported by the fact that serum provides more protein content and this apparent yield was slightly higher in SCM than in XSFM expansions.

Cell characterization after 3D cultures in either SCM or XSFM showed the preservation of MSC CQA defined by the International Society for Cell and Gene Therapy (ISCT),[64] as in all cases cells were able to demonstrate adherence to plastic, an MSC-specific surface antigen expression profile, and capacity for trilineage mesenchymal differentiation, in line with other studies.[16,23,32] Only CD105 expression was lower with SCM + EA conditions than the guideline value (≥95%), but was still highly positive (≥90%), meeting the acceptance criteria specified by other authors.[65] Similar and even greater decreases in CD105 expression can be expected after harvest from microcarriers[24,31,32,50,66] due to the enzymatic dissociation,[67] which in any case is a reversible phenomenon.[21] Moreover, no signs of senescence were associated with 3D dynamic cultivation either in the presence or absence of serum in the expansion media (CPD ≤ 28.7), concurring with previous studies reporting no senescence at passage 4 and approximately 28% of senescent cells at passage 10 (CDP ≈ 20 and 48, respectively).[68]

In summary, WJ-MSC readily expanded in 3D-cultures using both serum-containing and xeno- and serum-free media while preserving their immunophenotype and multipotency, with similar harvest yields resulting from 2D cultures. While better initial cell attachment, total cell yields and cell expansion fold can be obtained with SCM in 3D, XSFM showed better performance in 2D. This helped in defining microcarrier colonization and attachment efficiency as CPPs, assuming that inefficient and uneven cell distribution on microcarriers at this stage hampers the entire expansion and, consequently, the VCD recovered with XSFM. At the same time, this highlights the importance of performing both preliminary studies in 2D and proper 3D transition and process optimization before progressing to further ATMP development phases such as clinical trials. Overall, very high cell densities were obtained with both media, with a new estimated maximum of 1.47×10^9 cells harvested per manufacturing scale batch (2.4 L).

AUTHOR CONTRIBUTIONS

Alba López-Fernández, Víctor Garcia-Gragera, Martí Lecina, and Joaquim Vives conceived the study. Alba López-Fernández and Víctor Garcia-Gragera performed experiments, analyzed data and prepared the first draft. Martí Lecina and Joaquim Vives revised data and revised the manuscript. All authors read and approved the final manuscript.

ACKNOWLEDGEMENTS

The authors would like to acknowledge Drs. Núria Marí, David Horna and Miquel Costa (Aglaris Cell Ltd) for technical assistance and for kindly providing samples of microcarriers; Dr César del Rio (Miltenyi Biotec) for providing samples MSC-Brew GMP Medium, Dr. Ramiro Gisler (Fujifilm Irvine Scientific) for providing samples of PRIME-XV MSC Expansion XSFM, StemCell Technologies for providing samples of MesenCult-ACF Plus Medium and Reactiva SA for providing samples of MSC Nutristem XF Medium. We would also thank Irene Carreras-Sánchez for technical assistance with 2D cell cultures; Fátima Shettiyar, Mireia Lloret, Sílvia Torrents and Dr. Margarita Codinach (Laboratori Cel·lular, Banc de Sang i Teixits, Barcelona, Spain) for assistance with flow cytometry data acquisition and analysis of the immunophenotype characterization. This research has been cofunded by the Departament d'Universitats i Recerca from *Generalitat de Catalunya* and European Social Funds (ESF) [2022 FI_B 00198 and 2023 FI-2 00198] and internal funds from Banc de Sang i Teixits (internal call for RDI project Ref. I.2019.006.R; PI: Joaquim Vives). Research in JV's laboratory is developed in the context of Red Española de Terapias Avanzadas (TERAV, expedient no. RD21/0017/0022) funded by Instituto de Salud Carlos III (ISCIII) in the context of NextGenerationEU's Recovery, Transformation and Resilience Plan, and has been recognized as a Consolidated Research Group by Generalitat de Catalunya (2021-SGR-00877).

CONFLICT OF INTEREST STATEMENT

The authors have no conflict of interests to declare.

DATA AVAILABILITY STATEMENT

The data that support the findings of this study are available upon reasonable request to the corresponding authors.

ORCID

Alba López-Fernández https://orcid.org/0000-0001-6072-0294
Víctor Garcia-Gragera https://orcid.org/0000-0002-3372-2080
Martí Lecina https://orcid.org/0000-0002-8757-9902
Joaquim Vives https://orcid.org/0000-0001-9719-5235

REFERENCES

1. Naji, A., Eitoku, M., Favier, B., Deschaseaux, F., Rouas-Freiss, N., & Suganuma, N. (2019). Biological functions of mesenchymal stem cells and clinical implications. *Cellular and Molecular Life Sciences*, *76*, 3323–3348. https://doi.org/10.1007/s00018-019-03125-1
2. Ramezankhani, R., Torabi, S., Minaei, N., Madani, H., Rezaeiani, S., Hassani, S. N., Gee, A. P., Dominici, M., Silva, D. N., Baharvand, H., & Hajizadeh-Saffar, E. (2020). Two decades of global progress in authorized advanced therapy medicinal products: An emerging revolution

in therapeutic strategies. *Frontiers in Cell and Developmental Biology*, *8*, 547653. https://doi.org/10.3389/fcell.2020.547653

3. Fernández-Santos, M. E., Garcia-Arranz, M., Andreu, E. J., García-Hernández, A. M., López-Parra, M., Villarón, E., Sepúlveda, P., Fernández-Avilés, F., García-Olmo, D., Prosper, F., Sánchez-Guijo, F., Moraleda, J. M., & Zapata, A. G. (2022). Optimization of mesenchymal stromal cell (MSC) manufacturing processes for a better therapeutic outcome. *Frontiers in Immunology*, *13*, 918565. https://doi.org/10.3389/fimmu.2022.918565
4. Liau, L. L., Ruszymah, B. H. I., Ng, M. H., & Law, J. X. (2020). Characteristics and clinical applications of Wharton's jelly-derived mesenchymal stromal cells. *Current Research in Translational Medicine*, *68*(1), 5–16. https://doi.org/10.1016/j.retram.2019.09.001
5. Saleh, M., Vaezi, A. A., Aliannejad, R., Sohrabpour, A. A., Kiaei, S. Z. F., Shadnoush, M., Siavashi, V., Aghaghazvini, L., Khoundabi, B., Abdoli, S., Chahardouli, B., Seyhoun, I., Alijani, N., & Verdi, J. (2021). Cell therapy in patients with COVID-19 using Wharton's jelly mesenchymal stem cells: A phase 1 clinical trial. *Stem Cell Research & Therapy*, *12*, 410. https://doi.org/10.1186/s13287-021-02483-7
6. García-Muñoz, E., & Vives, J. (2021). Towards the standardization of methods of tissue processing for the isolation of mesenchymal stromal cells for clinical use. *Cytotechnology*, *73*, 513–522. https://doi.org/10.1007/s10616-021-00474-3
7. Jayaraman, P., Lim, R., Ng, J., & Vemuri, M. C. (2021). Acceleration of translational mesenchymal stromal cell therapy through consistent quality GMP manufacturing. *Frontiers in Cell and Developmental Biology*, *9*, 648472. https://doi.org/10.3389/fcell.2021.648472
8. Frontini-López, Y. R., Rivera, L., Aldana, A. A., Rivero, G., Liverani, L., Abraham, G. A., Boccaccini, A. R., Bustos, D. M., & Uhart, M. (2023). Human adipose mesenchymal stromal cells growing into PCL-nHA electrospun scaffolds undergo hypoxia adaptive ultrastructural changes. *Biotechnology Journal*, *18*(4), 2200413. https://doi.org/10.1002/biot.202200413
9. García-Fernández, C., López-Fernández, A., Borrós, S., Lecina, M., & Vives, J. (2020). Strategies for large-scale expansion of clinical-grade human multipotent mesenchymal stromal cells. *Biochemical Engineering Journal*, *159*, 107601. https://doi.org/10.1016/j.bej.2020.107601
10. Hulme, C. H., Mennan, C., McCarthy, H. S., Davies, R., Lan, T., Rix, L., Perry, J., & Wright, K. (2023). A comprehensive review of quantum bioreactor cell manufacture: Research and clinical applications. *Cytotherapy*, *25*(10), 1017–1026. https://doi.org/10.1016/j.jcyt.2023.04.004
11. Lembong, J., Kirian, R., Takacs, J. D., Olsen, T. R., Lock, L. T., Rowley, J. A., & Ahsan, T. (2020). Bioreactor parameters for microcarrier-based human MSC expansion under xeno-free conditions in a vertical-wheel system. *Bioengineering*, *7*(3), 73. https://doi.org/10.3390/bioengineering7030073
12. de Almeida Fuzeta, M., Bernardes, N., Oliveira, F. D., Costa, A. C., Fernandes-Platzgummer, A., Farinha, J. P., Rodrigues, C. A. V., Jung, S., Tseng, R. J., Milligan, W., Lee, B., Castanho, M. A. R. B., Gaspar, D., Cabral, J. M. S., & da Silva, C. L. (2020). Scalable production of human mesenchymal stromal cell-derived extracellular vesicles under serum-/xeno-free conditions in a microcarrier-based bioreactor culture system. *Frontiers in Cell and Developmental Biology*, *8*, 553444. https://doi.org/10.3389/fcell.2020.553444
13. Borys, B. S., Dang, T., So, T., Rohani, L., Revay, T., Walsh, T., Thompson, M., Argiropoulos, B., Rancourt, D. E., Jung, S., Hashimura, Y., Lee, B., & Kallos, M. S. (2021). Overcoming bioprocess bottlenecks in the large-scale expansion of high-quality hiPSC aggregates in vertical-wheel stirred suspension bioreactors. *Stem Cell Research & Therapy*, *12*, 55. https://doi.org/10.1186/s13287-020-02109-4
14. Timmins, N. E., Kiel, M., Günther, M., Heazlewood, C., Doran, M. R., Brooke, G., & Atkinson, K. (2012). Closed system isolation and scalable expansion of human placental mesenchymal stem cells. *Biotechnology and Bioengineering*, *109*(7), 1817–1826. https://doi.org/10.1002/bit.24425
15. Moreira, F., Mizukami, A., de Souza, L. E. B., Cabral, J. M. S., da Silva, C. L., Covas, D. T., & Swiech, K. (2020). Successful use of human AB serum to support the expansion of adipose tissue-derived mesenchymal stem/stromal cell in a microcarrier-based platform. *Frontiers in Bioengineering and Biotechnology*, *8*, 477316. https://doi.org/10.3389/fbioe.2020.00307
16. de Soure, A. M., Fernandes-Platzgummer, A., Moreira, F., Lilaia, C., Liu, S. H. H., Ku, C. P. P., Huang, Y. F. F., Milligan, W., Cabral, J. M. S. S., & da Silva, C. L. (2017). Integrated culture platform based on a human platelet lysate supplement for the isolation and scalable manufacturing of umbilical cord matrix-derived mesenchymal stem/stromal cells. *Journal of Tissue Engineering and Regenerative Medicine*, *11*(5), 1630–1640. https://doi.org/10.1002/term.2200
17. Lam, A. T. L., Li, J., Toh, J. P. W., Sim, E. J. H., Chen, A. K. Y., Chan, J. K., Choolani, M., Reuveny, S., Birch, W. R., & Oh, S. K. W (2017). Biodegradable poly-ε-caprolactone microcarriers for efficient production of human mesenchymal stromal cells and secreted cytokines in batch and fed-batch bioreactors. *Cytotherapy*, *19*(3), 419–432. https://doi.org/10.1016/j.jcyt.2016.11.009
18. Hupfeld, J., Gorr, I. H., Schwald, C., Beaucamp, N., Wiechmann, K., Kuentzer, K., Huss, R., Rieger, B., Neubauer, M., & Wegmeyer, H. (2014). Modulation of mesenchymal stromal cell characteristics by microcarrier culture in bioreactors. *Biotechnology and Bioengineering*, *111*(11), 2290–2302. https://doi.org/10.1002/bit.25281
19. Goh, T. K. P., Zhang, Z. Y., Chen, A. K. L., Reuveny, S., Choolani, M., Chan, J. K. Y., & Oh, S. K. W. (2013). Microcarrier culture for efficient expansion and osteogenic differentiation of human fetal mesenchymal stem cells. *BioResearch Open Access*, *2*(2), 84–97. https://doi.org/10.1089/biores.2013.0001
20. Sion, C., Ghannoum, D., Ebel, B., Gallo, F., Isla, N., Guedon, E., Chevalot, I., & Olmos, E. (2021). A new perfusion mode of culture for WJ-MSCs expansion in a stirred and online monitored bioreactor. *Biotechnology and Bioengineering*, *118*(11), 4453–4464. https://doi.org/10.1002/bit.27914
21. Campbell, A., Fernandes-Platzgummer, A., Andrade, P. Z., Gimble, J. M., Wen, Y., Boucher, S., Vemuri, M. C., & Cabral, M. S. (2014). A xenogeneic-free bioreactor system for the clinical-scale expansion of human mesenchymal stem/stromal cells. *Biotechnology and Bioengineering*, *111*(6), 1116–1127. https://doi.org/10.1002/bit.25187
22. Sion, C., Loubière, C., Wlodarczyk-Biegun, M. K., Davoudi, N., Müller-Renno, C., Guedon, E., Chevalot, I., & Olmos, E. (2020). Effects of microcarriers addition and mixing on WJ-MSC culture in bioreactors. *Biochemical Engineering Journal*, *157*, 107521. https://doi.org/10.1016/j.bej.2020.107521
23. Leber, J., Barekzai, J., Blumenstock, M., Pospisil, B., Salzig, D., & Czermak, P. (2017). Microcarrier choice and bead-to-bead transfer for human mesenchymal stem cells in serum-containing and chemically defined media. *Process Biochemistry*, *59*, 255–265. https://doi.org/10.1016/j.procbio.2017.03.017
24. Santos, F., Andrade, P. Z., Abecasis, M. M., Gimble, J. M., Chase, L. G., Campbell, A. M., Boucher, S., Vemuri, M. C., da Silva, C. L., & Cabral, J. M. S. (2011). Toward a clinical-grade expansion of mesenchymal stem cells from human sources: A microcarrier-based culture system under xeno-free conditions. *Tissue Engineering Part C: Methods*, *17*(12), 1201–1210. https://doi.org/10.1089/ten.tec.2011.0255
25. Su, Q., Ganesh, S., Moreno, M., Bommireddy, Y., Gonzalez, M., Reklaitis, G. V., & Nagy, Z. K. (2019). A perspective on Quality-by-Control (QbC) in pharmaceutical continuous manufacturing. *Computers & Chemical Engineering*, *125*, 216–231. https://doi.org/10.1016/j.compchemeng.2019.03.001
26. Karnieli, O., Friedner, O. M., Allickson, J. G., Zhang, N., Jung, S., Fiorentini, D., Abraham, E., Eaker, S. S., Yong, T. K., Chan, A., Griffiths, S., Wehn, A. K., Oh, S., & Karnieli, O. (2017). A consensus introduction

to serum replacements and serum-free media for cellular therapies. *Cytotherapy*, *19*(2), 155–169. https://doi.org/10.1016/j.jcyt.2016.11.011
27. Kunas, K. T., & Papoutsakis, E. T. (1990). The protective effect of serum against hydrodynamic damage of hybridoma cells in agitated and surface-aerated bioreactors. *Journal of Biotechnology*, *15*(1-2), 57–69. https://doi.org/10.1016/0168-1656(90)90051-C
28. Tan, K. Y., Teo, K. L., Lim, J. F. Y., Chen, A. K. L., Reuveny, S., & Oh, S. K. W. (2015). Serum-free media formulations are cell line–specific and require optimization for microcarrier culture. *Cytotherapy*, *17*(8), 1152–1165. https://doi.org/10.1016/j.jcyt.2015.05.001
29. Timsina, H., McTyer, J., Rao, R. R., & Almodovar, J. (2022). A comparative evaluation of layer-by-layer assembly techniques for surface modification of microcarriers used in human mesenchymal stromal cell manufacturing. *Biotechnology Journal*, *17*(8), 2100605. https://doi.org/10.1002/biot.202100605
30. Bin Hassan, M. N. F., Yazid, M. D., Yunus, M. H. M., Chowdhury, S. R., Lokanathan, Y., Idrus, R. B. H., Ng, A. M. H., & Law, J. X. (2020). Large-scale expansion of human mesenchymal stem cells. *Stem Cells International*, *2020*, 17. https://doi.org/10.1155/2020/9529465
31. Mizukami, A., Fernandes-Platzgummer, A., Carmelo, J. G., Swiech, K., Covas, D. T., Cabral, J. M. S., & da Silva, C. L. (2016). Stirred tank bioreactor culture combined with serum-/xenogeneic-free culture medium enables an efficient expansion of umbilical cord-derived mesenchymal stem/stromal cells. *Biotechnology Journal*, *11*(8), 1048–1059. https://doi.org/10.1002/biot.201500532
32. Tozetti, P. A., Caruso, S. R., Mizukami, A., Fernandes, T. R., da Silva, F. B., Traina, F., Covas, D. T., Orellana, M. D., & Swiech, K. (2017). Expansion strategies for human mesenchymal stromal cells culture under xeno-free conditions. *Biotechnology Progress*, *33*(5), 1358–1367. https://doi.org/10.1002/btpr.2494
33. Loubière, C., Sion, C., De Isla, N., Reppel, L., Guedon, E., Chevalot, I., & Olmos, E. (2019). Impact of the type of microcarrier and agitation modes on the expansion performances of mesenchymal stem cells derived from umbilical cord. *Biotechnology Progress*, *35*(6), e2887. https://doi.org/10.1002/btpr.2887
34. Noronha, N. C., Mizukami, A., Orellana, M. D., Oliveira, M. C., Covas, D. T., Swiech, K., & Malmegrim, K. C. R. (2021). Hypoxia priming improves in vitro angiogenic properties of umbilical cord derived-mesenchymal stromal cells expanded in stirred-tank bioreactor. *Biochemical Engineering Journal*, *168*, 107949. https://doi.org/10.1016/j.bej.2021.107949
35. Oliver-Vila, I., Coca, M. I., Grau-Vorster, M., Pujals-Fonts, N., Caminal, M., Casamayor-Genescà, A., Ortega, I., Reales, L., Pla, A., Blanco, M., García, J., & Vives, J. (2016). Evaluation of a cell-banking strategy for the production of clinical grade mesenchymal stromal cells from Wharton's jelly. *Cytotherapy*, *18*(1), 25–35. https://doi.org/10.1016/j.jcyt.2015.10.001
36. Zwietering, T. N. (1958). Suspending of solid particles in liquid by agitators. *Chemical Engineering Science*, *8*(3-4), 244–253. https://doi.org/10.1016/0009-2509(58)85031-9
37. Martínez-Monge, I., Comas, P., Catalán-Tatjer, D., Prat, J., Casablancas, A., Paredes, C., Lecina, M., & Cairó, J. J. (2020). The effect of the expression of the antiapoptotic BHRF1 gene on the metabolic behavior of a hybridoma cell line. *Applied Sciences*, *11*(14), 6258. https://doi.org/10.3390/app11146258
38. Oliver-Vila, I., Ramírez-Moncayo, C., Grau-Vorster, M., Marín-Gallén, S., Caminal, M., & Vives, J. (2018). Optimisation of a potency assay for the assessment of immunomodulative potential of clinical grade multipotent mesenchymal stromal cells. *Cytotechnology*, *70*, 31–44. https://doi.org/10.1007/s10616-017-0186-0
39. Poon, C. (2022). Measuring the density and viscosity of culture media for optimized computational fluid dynamics analysis of in vitro devices. *Journal of the Mechanical Behavior of Biomedical Materials*, *126*, 105024. https://doi.org/10.1016/j.jmbbm.2021.105024
40. Hunt, M. M., Meng, G., Rancourt, D. E., Gates, I. D., & Kallos, M. S. (2014). Factorial experimental design for the culture of human embryonic stem cells as aggregates in stirred suspension bioreactors reveals the potential for interaction effects between bioprocess parameters. *Tissue Engineering Part C: Methods*, *20*(1), 76–89. https://doi.org/10.1089/ten.tec.2013.0040
41. Doran, P. M. (2013). *Bioprocess engineering principles* (2nd ed.). Academic Press. https://doi.org/10.1016/c2009-0-22348-8
42. Silva Couto, P., Rotondi, M. C., Bersenev, A., Hewitt, C. J., Nienow, A. W., Verter, F., & Rafiq, Q. A. (2020). Expansion of human mesenchymal stem/stromal cells (hMSCs) in bioreactors using microcarriers: Lessons learnt and what the future holds. *Biotechnology Advances*, *45*, 107636. https://doi.org/10.1016/j.biotechadv.2020.107636
43. Wu, X., Kang, H., Liu, X., Gao, J., Zhao, K., & Ma, Z. (2016). Serum and xeno-free, chemically defined, no-plate-coating-based culture system for mesenchymal stromal cells from the umbilical cord. *Cell Proliferation*, *49*, 579–588. https://doi.org/10.1111/cpr.12279
44. Hoang, V. T., Trinh, Q. M. M., Phuong, D. T. M., Bui, H. T. H., Hang, L. M., Ngan, N. T. H., Anh, N. T. T., Nhi, P. Y., Nhung, T. T. H., Lien, H. T., Nguyen, T. D., Thanh, L. N., & Hoang, D. M. (2021). Standardized xeno- and serum-free culture platform enables large-scale expansion of high-quality mesenchymal stem/stromal cells from perinatal and adult tissue sources. *Cytotherapy*, *23*(1), 88–99. https://doi.org/10.1016/j.jcyt.2020.09.004
45. de Soure, A. M., Fernandes-Platzgummer, A., da Silva, C. L., & Cabral, J. M. S. (2016). Scalable microcarrier-based manufacturing of mesenchymal stem/stromal cells. *Journal of Biotechnology*, *236*, 88–109. https://doi.org/10.1016/j.jbiotec.2016.08.007
46. Badenes, S. M., Fernandes-Platzgummer, A., Rodrigues, C. A. V., Diogo, M. M., da Silva, C. L., & Cabral, J. M. S. (2015). Chapter 4: Microcarrier culture systems for stem cell manufacturing. In: *Stem Cell Manufacturing*, 77–104. https://doi.org/10.1016/B978-0-444-63265-4.00004-2
47. Ferrari, C., Balandras, F., Guedon, E., Olmos, E., Chevalot, I., & Marc, A. (2012). Limiting cell aggregation during mesenchymal stem cell expansion on microcarriers. *Biotechnology Progress*, *28*(3), 780–787. https://doi.org/10.1002/btpr.1527
48. Tsai, A. C., Jeske, R., Chen, X., Yuan, X., & Li, Y. (2020). Influence of microenvironment on mesenchymal stem cell therapeutic potency: From planar culture to microcarriers. *Frontiers in Bioengineering and Biotechnology*, *8*, 543936. https://doi.org/10.3389/fbioe.2020.00640
49. Heathman, T. R. J., Nienow, A. W., Rafiq, Q. A., Coopman, K., Kara, B., & Hewitt, C. J. (2018). Agitation and aeration of stirred-bioreactors for the microcarrier culture of human mesenchymal stem cells and potential implications for large-scale bioprocess development. *Biochemical Engineering Journal*, *136*, 9–17. https://doi.org/10.1016/j.bej.2018.04.011
50. Eibes, G., dos Santos, F., Andrade, P. Z., Boura, J. S., Abecasis, M. M. A., da Silva, C. L., & Cabral, J. M. S. (2010). Maximizing the ex vivo expansion of human mesenchymal stem cells using a microcarrier-based stirred culture system. *Journal of Biotechnology*, *146*(4), 194–197. https://doi.org/10.1016/j.jbiotec.2010.02.015
51. Hewitt, C. J., Lee, K., Nienow, A. W., Thomas, R. J., Smith, M., & Thomas, C. R. (2011). Expansion of human mesenchymal stem cells on microcarriers. *Biotechnology Letters*, *33*, 2325–2335. https://doi.org/10.1007/s10529-011-0695-4
52. Sun, L. Y., Hsieh, D. K., Syu, W. S., Li, Y. S., Chiu, H. T., & Chiou, T. W. (2010). Cell proliferation of human bone marrow mesenchymal stem cells on biodegradable microcarriers enhances in vitro differentiation potential. *Cell Proliferation*, *43*(5), 445–456. https://doi.org/10.1111/j.1365-2184.2010.00694.x
53. Elseberg, C. L., Leber, J., Salzig, D., Wallrapp, C., Kassem, M., Kraume, M., & Czermak, P. (2012). Microcarrier-based expansion process for hMSCs with high vitality and undifferentiated

characteristics. *International Journal of Artificial Organs*, *35*(2), 93–107. https://doi.org/10.5301/ijao.5000077

54. López-Fernández, A., Codinach, M., Coca, M. I., Prat-Vidal, C., Castaño, J., Torrents, S., Aran, G., Rodríguez, L., Querol, S., & Vives, J. (2023). Comparability exercise of critical quality attributes of clinical-grade human mesenchymal stromal cells from the Wharton's jelly: Single-use stirred tank bioreactors versus planar culture systems. *Cytotherapy*, *S1465-3249*(23), 01039–01043. https://doi.org/10.1016/j.jcyt.2023.08.008
55. Haack-Sørensen, M., Juhl, M., Follin, B., Harary Søndergaard, R., Kirchhoff, M., Kastrup, J., & Ekblond, A. (2018). Development of large-scale manufacturing of adipose-derived stromal cells for clinical applications using bioreactors and human platelet lysate. *Scandinavian Journal of Clinical and Laboratory Investigation*, *78*(4), 293–300. https://doi.org/10.1080/00365513.2018.1462082
56. Acosta, M. L., Sánchez, A., García, F., Contreras, A., & Molina, E. (2007). Analysis of kinetic, stoichiometry and regulation of glucose and glutamine metabolism in hybridoma batch cultures using logistic equations. *Cytotechnology*, *54*, 189–200. https://doi.org/10.1007/s10616-007-9089-9
57. Christie, A., & Butler, M. (1994). Glutamine-based dipeptides are utilized in mammalian cell culture by extracellular hydrolysis catalyzed by a specific peptidase. *Journal of Biotechnology*, *37*(3), 277–290. https://doi.org/10.1016/0168-1656(94)90134-1
58. Schop, D., Janssen, F. W., van Rijn, L. D. S., Fernandes, H., Bloem, R. M., de Bruijn, J. D., & van Dijkhuizen-Radersma, R. (2009). Growth, metabolism, and growth inhibitors of mesenchymal stem cells. *Tissue Engineering Part A*, *15*(8), 1877–1886. https://doi.org/10.1089/ten.tea.2008.0345
59. Cunha, B., Aguiar, T., Carvalho, S. B., Silva, M. M., Gomes, R. A., Carrondo, M. J. T., Gomes-Alves, P., Peixoto, C., Serra, M., & Alves, P. M. (2017). Bioprocess integration for human mesenchymal stem cells: From up to downstream processing scale-up to cell proteome characterization. *Journal of Biotechnology*, *248*, 87–98. https://doi.org/10.1016/j.jbiotec.2017.01.014
60. Heiden, M. G. V., Cantley, L. C., & Thompson, C. B. (2009). Understanding the Warburg Effect: The metabolic requirements of cell proliferation. *Science*, *324*(5930), 1029–1033. https://doi.org/10.1126/science.1160809
61. Tohyama, S., Fujita, J., Hishiki, T., Matsuura, T., Hattori, F., Ohno, R., Kanazawa, H., Seki, T., Nakajima, K., Kishino, Y., Okada, M., Hirano, A., Kuroda, T., Yasuda, S., Sato, Y., Yuasa, S., Sano, M., Suematsu, M., & Fukuda, K. (2016). Glutamine oxidation is indispensable for survival of human pluripotent stem cells. *Cell Metabolism*, *23*(4), 663–674. https://doi.org/10.1016/j.cmet.2016.03.001
62. Rafiq, Q. A., Brosnan, K. M., Coopman, K., Nienow, A. W., & Hewitt, C. J. (2013). Culture of human mesenchymal stem cells on microcarriers in a 5 L stirred-tank bioreactor. *Biotechnology Letters*, *35*, 1233–1245. https://doi.org/10.1007/s10529-013-1211-9
63. Gupta, P., Geris, L., Luyten, F. P., & Papantoniou, I. (2018). An integrated bioprocess for the expansion and chondrogenic priming of human periosteum-derived progenitor cells in suspension bioreactors. *Biotechnology Journal*, *13*(2), 1700087. https://doi.org/10.1002/biot.201700087
64. Dominici, M., Le Blanc, K., Mueller, I., Slaper-Cortenbach, I., Marini, F., Krause, D. S., Deans, R. J., Keating, A., Prockop, D. J., & Horwitz, E. M. (2006). Minimal criteria for defining multipotent mesenchymal stromal cells. The International Society for Cellular Therapy position statement. *Cytotherapy*, *8*(4), 315–317. https://doi.org/10.1080/14653240600855905
65. Codinach, M., Blanco, M., Ortega, I., Lloret, M., Reales, L., Coca, M. I., Torrents, S., Doral, M., Oliver-Vila, I., Requena-Montero, M., Vives, J., & Garcia-López, J. (2016). Design and validation of a consistent and reproducible manufacture process for the production of clinical-grade bone marrow–derived multipotent mesenchymal stromal cells. *Cytotherapy*, *18*(9), 1197–1208. https://doi.org/10.1016/j.jcyt.2016.05.012
66. Van Beylen, K., Papantoniou, I., & Aerts, J. M. (2021). Microcarrier screening and evaluation for dynamic expansion of human periosteum-derived progenitor cells in a xenogeneic free medium. *Frontiers in Bioengineering and Biotechnology*, *9*, 624890. https://doi.org/10.3389/fbioe.2021.624890
67. Potapova, I. A., Brink, P. R., Cohen, I. S., & Doronin, S. V. (2008). Culturing of human mesenchymal stem cells as three-dimensional aggregates induces functional expression of CXCR4 that regulates adhesion to endothelial cells. *The Journal of biological chemistry*, *283*(19), 13100–13107. https://doi.org/10.1074/jbc.M800184200
68. Cheng, H., Qiu, L., Ma, J., Zhang, H., Cheng, M., Li, W., Zhao, X., & Liu, K. (2011). Replicative senescence of human bone marrow and umbilical cord derived mesenchymal stem cells and their differentiation to adipocytes and osteoblasts. *Molecular Biology Reports*, *38*, 5161–5168. https://doi.org/10.1007/s11033-010-0665-2

How to cite this article: López-Fernández, A., Garcia-Gragera, V., Lecina, M., & Vives, J. (2024). Identification of critical process parameters for expansion of clinical grade human Wharton's jelly-derived mesenchymal stromal cells in stirred-tank bioreactors. *Biotechnology Journal*, *19*, e2300381. https://doi.org/10.1002/biot.202300381